The Journal of Immunology

Fatty Acids from Very Low-Density Lipoprotein Lipolysis Products Induce Lipid Droplet Accumulation in Human Monocytes

Laura J. den Hartigh, Jaime E. Connolly-Rohrbach, Samantha Fore, Thomas R. Huser and John C. Rutledge

J Immunol 2010; 184:3927-3936; Prepublished online 5 March 2010;
doi: 10.4049/jimmunol.0903475
http://www.jimmunol.org/content/184/7/3927

The Journal of Immunology is published twice each month by
The American Association of Immunologists, Inc.,
1451 Rockville Pike, Suite 650, Rockville, MD 20852

Print ISSN: 0022-1767 Online ISSN: 1550-6606.

Fatty Acids from Very Low-Density Lipoprotein Lipolysis Products Induce Lipid Droplet Accumulation in Human Monocytes

Laura J. den Hartigh,*,†,[1] Jaime E. Connolly-Rohrbach,*,‡,[1] Samantha Fore,*,§ Thomas R. Huser,*,§ and John C. Rutledge*

One mechanism by which monocytes become activated postprandially is by exposure to triglyceride-rich lipoproteins such as very low-density lipoproteins (VLDL). VLDL are hydrolyzed by lipoprotein lipase at the blood-endothelial cell interface, releasing free fatty acids. In this study, we examined postprandial monocyte activation in more detail, and found that lipolysis products generated from postprandial VLDL induce the formation of lipid-filled droplets within cultured THP-1 monocytes, characterized by coherent antistokes Raman spectroscopy. Organelle-specific stains revealed an association of lipid droplets with the endoplasmic reticulum, confirmed by electron microscopy. Lipid droplet formation was reduced when lipoprotein lipase-released fatty acids were bound by BSA, which also reduced cellular inflammation. Furthermore, saturated fatty acids induced more lipid droplet formation in monocytes compared with mono- and polyunsaturated fatty acids. Monocytes treated with postprandial VLDL lipolysis products contained lipid droplets with more intense saturated Raman spectroscopic signals than monocytes treated with fasting VLDL lipolysis products. In addition, we found that human monocytes isolated during the peak postprandial period contain more lipid droplets compared with those from the fasting state, signifying that their development is not limited to cultured cells but also occurs in vivo. In summary, circulating free fatty acids can mediate lipid droplet formation in monocytes and potentially be used as a biomarker to assess an individual's risk of developing atherosclerotic cardiovascular disease. ***The Journal of Immunology*****, 2010, 184: 3927–3936.**

Understanding interactions between circulating monocytes and lipoproteins is currently an area of active investigation related to inflammatory diseases such as atherosclerosis (1, 2). Triglyceride (TG)-rich lipoproteins, such as very low-density lipoproteins (VLDL), are commonly regarded as proinflammatory (3). VLDL, which are generated by the liver, are hydrolyzed by lipoprotein lipase (LpL) anchored to endothelial cells, resulting in the release of free fatty acids, phospholipids, monoglycerides, and diglycerides and the conversion of VLDL into remnant lipoproteins. This process is enhanced postprandially and can induce cellular injury in neighboring endothelial cells and monocytes (4). Such inflammatory injury can result in increased monocyte activation and recruitment to the arterial intima, contributing to foam cell development and fatty streak formation characteristic of atherosclerotic cardiovascular disease (ASCVD).

Excessive lipid accumulation within cells is a central feature of some metabolic diseases such as atherosclerosis, but little is known about the role that cytoplasmic lipid droplets play in monocyte responses to hypertriglyceridemia. Lipid droplets are commonly found in adipocytes, but exist in virtually all types of cells when faced with lipid overload. In nonadipocytes, lipid droplets are believed to function as lipid storage sites for later β-oxidation, membrane biogenesis, hormone synthesis, and other cellular functions (5). Recently, more diverse functions of the lipid droplet have been discovered largely related to intracellular signaling, protein storage, as well as protein degradation (6–9). Lipid droplets typically consist of a core of neutral lipids composed of TGs, cholesterol esters, and fatty acids, surrounded by a phospholipid monolayer (10, 11). It has been suggested that lipid droplets originate from the endoplasmic reticulum (ER), as they have been found in close proximity to ER membranes and contain a similar phospholipid profile as the ER (12, 13). The molecular composition, cell-specific function, and biogenesis of the lipid droplet are intense areas of investigation and currently remain unknown.

Prevention of lipid overload may be important in the prevention of metabolic disease states. A new unified view of lipid droplets as distinct organelles with the ability to store excess lipids and to participate in specific intracellular signaling cascades related to the energy requirements of the cell (14), makes them attractive targets for investigation. In this study, monocyte treatment with VLDL lipolysis products generated by treating VLDL with LpL resulted in the formation of cytoplasmic lipid structures, which led us to examine their origins in more detail. We determined that the droplets

*Division of Endocrinology, Clinical Nutrition, and Vascular Medicine, Department of Internal Medicine, †Division of Pathology, Microbiology, and Immunology, Department of Veterinary Medicine, ‡Department of Cell Biology and Human Anatomy, and §Center for Biophotonics Science and Technology, University of California, Davis, Davis, CA 95616.

[1]L.J.d.H. and J.E.C.-R. contributed equally to this work.

Received for publication October 28, 2009. Accepted for publication January 16, 2010.

This work was supported by a graduate fellowship from the Center for Biophotonics Science and Technology (Sacramento, CA) and National Heart, Lung, and Blood Insitute Grant HL055667. This work was also supported in part by funding for the American Heart Association through a Grant-in-Aid (to T.H.) and by the National Science Foundation. The Center for Biophotonics and National Science Foundation Science and Technology Center is managed by the University of California, Davis, under Cooperative Agreement No. PHY 0120999. Support is also acknowledged from the Clinical Translational Science Center under grant number UL1 RR024146 from the National Center for Research Resources, a component of the National Institutes of Health, and the National Institutes of Health Roadmap for Medical Research.

Address correspondence and reprint requests to Dr. Laura J. den Hartigh, University of California, Davis, VM3A Room 4206, One Shields Avenue, Davis, CA 95616. E-mail address: ljhiggins@ucdavis.edu

The online version of this article contains supplemental material.

Abbreviations used in this paper: ASCVD, atherosclerotic cardiovascular disease; a.u., arbitrary units; CARS, coherent anti-Stokes Raman scattering; DIC, differential interference contrast; ER, endoplasmic reticulum; FVLDL, fasting VLDL; LD, lipid droplet; LpL, lipoprotein lipase; PVLDL, postprandial VLDL; TEM, transmission electron microscopy; TG, triglyceride; VLDL, very low-density lipoprotein.

were indeed lipid-filled and that fatty acids were partially responsible for this lipid droplet formation. In addition, there appears to be a correlation between VLDL lipolysis product-induced cytokine synthesis and lipid droplet formation. Organelle-specific stains indicated that in monocytes, as has been observed in other cell types, the lipid droplets associate with the ER, a finding we confirmed by transmission electron microscopy (TEM). Furthermore, monocyte treatment with postprandial VLDL (PVLDL) lipolysis products resulted in the formation of lipid droplets with more intense saturated Raman spectroscopic modes, whereas fasting VLDL (FVLDL) lipolysis product-treated monocytes contained lipid droplets exhibiting higher unsaturated lipid modes. Similar lipid droplets were found in fresh human monocytes isolated from postprandial whole blood. Our study presents novel observations that lipolysis products generated from VLDL induce the rapid formation of cytoplasmic lipid droplets within naive monocytes in vitro, and freshly isolated primary postprandial monocytes contain similar lipid structures, observations that may be clinically important. Thus, lipid droplet formation by postprandially activated monocytes appears to be a potential mechanism of lipotoxic protection but additionally results in monocyte inflammation, which has been linked to vascular inflammation and ASCVD.

Materials and Methods

Monocyte cell culture and treatment conditions

THP-1 human monocytes were purchased from American Type Culture Collection (Manassas, VA) and maintained in suspension between 5×10^4 and 8×10^5 cells/ml in RPMI 1640 medium supplemented with 2 mM L-glutamine and containing 10 mM HEPES, 1 mM sodium pyruvate, 4.5 g/l glucose, 1.5 g/l bicarbonate, 10% FBS, and 0.05 mM 2-ME. Monocytes were incubated in 5% CO_2 and 95% O_2 at 37˚C during growth and treatment. THP-1 monocyte treatments were conducted at a cell density of 1×10^6 cells/ml for the times indicated. Monocyte viability was monitored after all treatments using trypan blue exclusion, and remained >90% for all treatments. Prior to cell treatment, lipolysis of VLDL was performed by incubating VLDL (200 mg TG/dl) with bovine LpL (2 U/ml, Sigma-Aldrich, St. Louis, MO) for 30 min at 37˚C. In some experiments, fatty-acid free BSA (60 mg/ml, Sigma-Aldrich) was added to each lipid treatment 5 min prior to exposure to the cells. In other experiments, THP-1 cells were treated with the synthetic fatty acids linoleic acid (Cayman Chemical, Ann Arbor, MI), oleic acid (Sigma-Aldrich), stearic acid (Cayman Chemical), and palmitic acid (Nu-Check Prep, Elysian, MN), at 150 μM each, for 3 h. In all experiments, THP-1 monocytes were treated at a cell density of 1×10^6 cells/ml for the times indicated. Lipid droplets were confirmed by differential interference contrast (DIC) microscopy using a 40× objective or phase-contrast microscopy using a 60× objective. For some experiments, human PBMCs were isolated by centrifuging buffy coats over a Lymphosep density solution (ρ = 1.07, MP Biomedicals, Solon, OH) for 20 min, washed three times, and immediately processed for quantitative RT-PCR. All THP-1 monocytes, freshly isolated human monocytes, and PBMCs used in these experiments were maintained in an undifferentiated state.

VLDL isolation

Male and female healthy human volunteers ages 18–55 y were recruited from the University of California, Davis campus. The study was approved by the Human Subjects Research Committee of the University of California, Davis. The study aims and protocol were explained to each participant and informed written consent was obtained. All studies were performed at the same time of day to eliminate any diurnal variables. Blood was drawn by venipuncture from subjects before and 3.5 h after consumption of a moderately high-fat meal [40% calories from fat, as described previously (3)] into K_2-EDTA vacutainer tubes and centrifuged at 1200*g* for 10 min to obtain cell-free plasma. Plasma was treated with 0.01% sodium azide as a preservative and subjected to lipoprotein isolation as described previously (15), with minor modifications. Chylomicrons were removed from postprandial plasma by centrifuging for 30 min at 63,000*g* prior to VLDL isolation. VLDL samples from multiple donors were pooled together and dialyzed overnight at 4˚C in 0.9% NaCl and 0.01% EDTA and quantified for total TG content using a kit from Sigma-Aldrich. Lipolysis of VLDL was induced by the addition of bovine LpL (Sigma-Aldrich) at 2 U/ml for 30 min at 37˚C, where indicated.

Oil Red O staining

THP-1 human monocytes (1×10^6 cells/ml) were treated with VLDL (200 mg TG/dl), LpL (2 U/ml), or VLDL lipolysis products generated as described previously for 3 h at 37˚C. Cells were harvested after treatment, washed one time with PBS without calcium chloride and magnesium chloride, and resuspended in 1% paraformaldehyde for fixation. After incubation at room temperature for 30 min, the cells were collected, washed one time with deionized water, and resuspended in 60% isopropanol for 5 min. The isopropanol was removed, the cells were resuspended in Oil Red O stain (Lonza, Walkersville, MD), and incubated at room temperature for 5 min. After staining, the cells were washed several times with deionized water to remove excess stain, resuspended in 20 μl deionized water, and viewed using DIC, phase contrast, or epifluorescence microscopy.

Coherent anti-Stokes Raman scattering imaging of monocyte lipid droplets

To analyze lipid-filled droplets in living monocytes, we used a custom-built coherent anti-Stokes Raman scattering (CARS) microscopy system. A 1064 nm Nd:YVO_4 laser (PicoTrain, HighQ Laser) with 7 ps pulse width and 76 mHz repetition rate is used as the Stokes pulse to generate the CARS signal and also serves as the pump laser for an Optical Parametric Oscillator (OPO, Levante, APE-Berlin, Germany). The tunable OPO with a wavelength range between 790–920 nm provides the pump pulse for the CARS signal generation. Both beams are spatially and temporally overlapped and combined by a 970 nm dichroic mirror. To diminish potential photo damage to the cells, the laser repetition rate is reduced 10-fold to 7.6 mHz by an electro-optical modulator (Conoptics, Danbury, CT). The combined laser beams are sent into an inverted optical microscope (IX71, Olympus America, Center Valley, PA) and focused to a diffraction-limited spot by a 60× oil objective (Olympus America). The forward-directed CARS signal generated in the sample is separated from the laser beams by a dichroic mirror and a multi-photon short-pass filter (Semrock, Rochester, NY) and is then collected by a single photon counting avalanche photodiode detector (APD, SPCM-AQR 14, Perkin-Elmer, Wellesley, MA). The APD signal is processed using time-correlated single photon counting electronics (TimeHarp200, PicoQuant GmbH, Adlershof, Germany) and displayed using image acquisition and analysis software (SymPhoTime, PicoQuant GmbH).

To image lipid droplets in primary monocytes, the OPO beam was tuned to 816 nm and serves as the pump laser, whereas the 1064 nm line of the Nd:YVO_4 laser was used as the Stokes probe beam. Together, the two beams coherently probe the strong aliphatic lipid CH stretch vibration at 2854 cm^{-1}, which results in the generation of a strong CARS signal at 661 nm. Images are acquired at 256 × 256 pixels with an acquisition time of 1 min/image.

In vitro LysoTracker, MitoTracker, and ER-Tracker analysis

THP-1 human monocytes (1×10^6 cells/ml) were treated with VLDL lipolysis products generated as described previously for 3 h at 37˚C. After treatment, cells were stained with LysoTracker Red DND-99 (50 nM final concentration; Molecular Probes, Eugene, OR), MitoTracker Green FM (50 nM final concentration; Molecular Probes), or ER-Tracker Red (100 nM final concentration; Molecular Probes). Cells stained with ER-Tracker Red were then fixed in 1% paraformaldehyde for 2 min at 37˚C, washed, and resuspended in 20 μl probe-free medium. Localization of the Tracker dyes was examined by FITC or rhodamine optical filters on a Zeiss Axioskop 2 plus fluorescence microscope.

TEM

THP-1 human monocytes (1×10^6 cells/ml) were treated with VLDL lipolysis products generated as described previously for either 30 min or 3 h at 37˚C. At each time point, 1 ml cells were harvested and fixed by resuspension in modified Karnovsky's fixative (2% paraformaldehyde and 2.5% glutaraldehyde in 0.06 M Sorenson's phosphate buffer, pH 7.2). Cells were washed in Sorenson's phosphate buffer three times for 1 min each, resuspended in 2% OSO_4 (osmium tetroxide), and incubated at 4˚C for 1 h. Prior to dehydration, the cells were washed in distilled water three times for 1 min each at 4˚C. Samples were dehydrated through serial washes in graded acetone (10 min each). The dehydrated samples were embedded in epoxy resin and ultra-thin sections were obtained after heavy metal staining. The images were collected on a Phillips CM120 microscope at 80 kV.

Quantitative real-time RT-PCR

Gene expression of inflammatory cytokines from treated monocytes was examined using quantitative real-time RT-PCR as described previously (16). Briefly, RNA was extracted from treated THP-1 cells using TRIzol reagent (Invitrogen, San Diego, CA) and an RNeasy mini kit (Qiagen, Valencia,

CA). Total RNA (5 μg) was converted to cDNA using a Superscript III kit (Invitrogen). Quantification of mRNA from gene transcripts of TNF-α, IL-1β, IL-8, and β-actin was performed using the GeneAmp 7900 HT sequence detection system (Applied Biosystems, Foster City, CA), as described previously (17). Primers for the genes of interest were designed using Primer Express (Applied Biosystems) and synthesized by Integrated DNA Technologies. The primer sequences were as follows: TNF-α (sense, 5′-AACATCCAACCTTCCCAAACG-3′; antisense, 5′-CCCTAAGCCCCCAATTCTCTT-3′), IL-1β (sense, 5′-AATTTGAGTCTGCCCAGTTCCC-3′; antisense, 5′-AGTCAGTTATATCCTGGCCGCC-3′), IL-8 (sense, 5′-GAGAAATCAGGAAGGCTGCC-3′; antisense, 5′-ACATGACTTCCAAGCTGGCC-3′), and β-actin (sense, 5′-CTGTCCACCTTCCAGCAGATGT-3′; antisense, 5′-CGCAACTAAGTCATAGTCCGCC-3′). Expression of TNF-α, IL-1β, and IL-8 were normalized to β-actin and represented in terms of a fold change.

TNF-α ELISA

Secreted TNF-α protein from treated THP-1 monocytes was quantified using a human ELISA kit, according to the manufacturer's instructions (BD Biociences, San Jose, CA).

Spontaneous Raman spectroscopy of single lipid droplets in monocytes

Spontaneous Raman spectra of single lipid droplets within monocytes were acquired on a custom-built inverted laser-tweezers Raman microscope. The main microscope platform consists of an Olympus IX-71 microscope equipped with a 100×, NA 1.4, oil immersion objective optimized for near-infrared operation (Olympus America). The laser source is an 80 mW, 785 nm diode-pumped solid-state laser (Crystalaser, Reno, NV). The spontaneously scattered Raman-shifted light is collected by the same microscope objective, dispersed by an imaging spectrograph (SP2300i, Roper Scientific, Trenton, NJ), equipped with a 300 lines/mm grating, and detected with a back-illuminated, thermoelectrically cooled deel-depletion charge-coupled device camera with 1340 × 1000 pixels (PIXIS 100BR, Roper Scientific). To acquire spectra from individual lipid droplets in monocytes, the monocytes were optically trapped by their cytoplasmic lipid droplets using the highly focused near-infrared laser beam. This immobilizes the cell and allows us to obtain full Raman spectra within 30–60 s signal acquisition time. Background spectra were acquired from the buffer solution, while avoiding trapping any cells. After the subtraction of the individual background spectra, the resulting spectra were processed equally, including baseline subtraction and peak area normalization.

Analysis of lipid droplets in human monocytes

Buffy coats were isolated from blood drawn during the fasting and peak postprandial periods. Contaminating erythrocytes were removed using a lysing solution (BD Biosciences). Monocytes within the buffy coats were labeled with an Alexa488-conjugated CD14 Ab, cells were fixed using 1% paraformaldehyde, and then stained with Oil Red O as described previously. Cells were imaged with a personal DV deconvolution microscope (Applied Precision, Issaquiah, WA) using a 40× objective. A FITC filter was used for excitation of the Alexa-488 and Oil Red O, and emission profiles at 528 nm and 617 nm were used to detect CD14 and Oil Red O, respectively. A minimum of 40 frames of cells were captured per sample. Images were deconvolved using Δ Vision software, giving a partially computer-generated final image. Total monocytes with and without lipid droplets were counted from samples isolated from the fasting state and the peak postprandial period, and presented as a percentage of monocytes positive for lipid droplets. In addition, total TGs and NEFAs were measured from the corresponding plasma samples using kits from Sigma-Aldrich and Wako Chemicals, respectively, according to the manufacturers' instructions.

Statistics analysis

All statistical analyses were performed using Student *t* test or one-way ANOVA, where appropriate, with SigmaStat software. All data are presented as the mean ± SEM. Statistical significance was reported for $p < 0.05$.

Results

Treatment of THP-1 monocytic cells with VLDL lipolysis products induces lipid droplet biogenesis

Initial studies revealed that THP-1 cells develop intracellular droplet-like structures after a 3-h treatment with VLDL lipolysis products, generated by pretreating VLDL with LpL. DIC microscopy was used to visualize the droplet-like structures in the VLDL

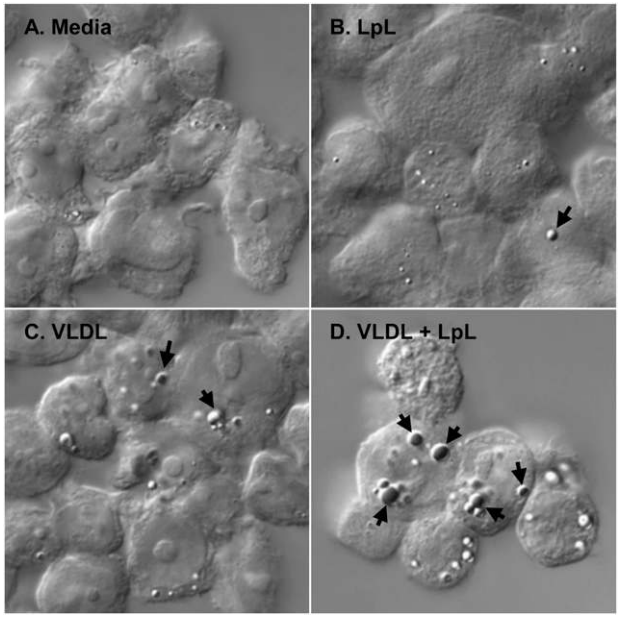

FIGURE 1. VLDL lipolysis product-induced droplets are lipid-filled. THP-1 monocytes were treated at a cell density of 1×10^6 cells/ml for 3 h. Monocytes were fixed in 1% paraformaldehyde and lipid droplets were stained with Oil Red O. Monocytes were observed at room temperature using a Zeiss Axioskop2 plus microscope with a *Pan*-Neofluar 40× objective, 1.3 oil. DIC images were captured using a Zeiss AxioCam MRm camera and processed using AxioVision LE software. *A–C*, Negative controls included (*A*) media, (*B*) LpL (2 U/ml), and (*C*) VLDL alone (200 mg TG/dl), and resulted in low levels of droplet formation. *D*, VLDL lipolysis products (200 mg TG/dl VLDL and 2 U/ml LpL) induced formation of droplets that stained red with Oil Red O, indicating that they are lipid filled. Cells from each treatment were analyzed over a minimum of 10 frames per experiment. The experiment was repeated three times, with similar results. Arrows, lipid droplets. Original magnification ×400 for all panels.

lipolysis product-treated cells (Fig. 1*D*, arrows). Cells were stained with Oil Red O, which stains neutral lipids, to confirm that the droplets are lipid filled. Untreated THP-1 monocytes (Fig. 1*A*) and monocytes treated with LpL (Fig. 1*B*) or VLDL alone (Fig. 1*C*) contained very few droplets. Supplemental Fig. 1 represents DIC microscopic images of treated cells without Oil Red O staining, to confirm that the lipid droplet formation is not an artifact of the Oil Red O staining procedure.

To further confirm that lipid-filled droplets exist in living monocytes and to avoid potential artifacts from fixation or Oil Red O staining, we also imaged treated THP-1 monocytes by CARS microscopy. CARS microscopy is a label-free chemical imaging technique suitable for live cell microscopy that probes specific molecular vibrations by inelastic light scattering. Here, we tuned our system to probe the aliphatic CH vibration at 2845 cm^{-1} that is common to all lipids (Fig. 2*A*). Images obtained by this technique are similar to confocal fluorescence microscopy images, but are based on the intrinsic contrast between these specific molecular vibrations. As shown in the CARS image in Fig. 2*B*, only lipid droplets within the cytoplasm of a monocyte produce visible contrast using this modality, which further underscores the highly localized lipid storage in these cells. The lipid droplets imaged in this cell are all of approximately the same size and similar overall lipid density.

VLDL lipolysis product-induced lipid droplets appear to be in close proximity to the ER

Lipid droplets can form within cells by several processes, but they most commonly originate from the ER. To determine whether VLDL lipolysis product-induced lipid droplets are associated with ER

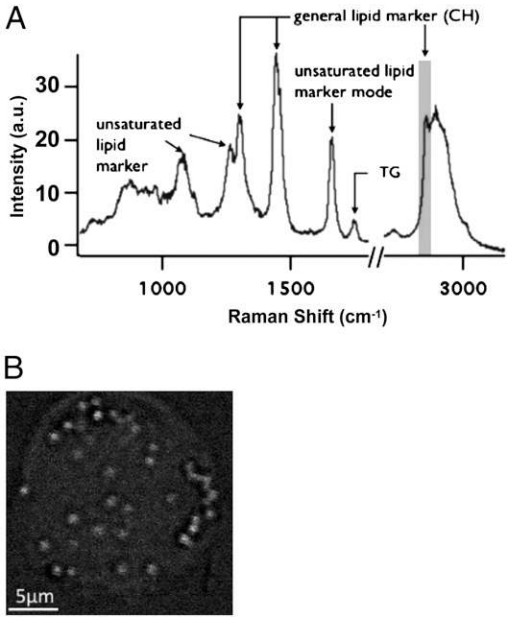

FIGURE 2. CARS imaging of THP-1 monocytes confirms the lipid nature of the droplets. After a 3-h treatment with VLDL and LpL (200 mg TG/dl, 2 U/ml), THP-1 monocytes were analyzed and imaged by CARS microscopy. *A*, Raman spectra obtained from individual lipid droplets inside monocytes exhibit all the hallmarks of lipids. *B*, A chemical image obtained by using the general lipid marker mode of an aliphatic CH vibration at 2845 cm^{-1} to generate the contrast confirms that the droplets inside monocytes are highly enriched in lipids. Lipid droplets are ~1 μm in diameter throughout the cell. Images and spectra were obtained on home-built instruments using and Olympus IX71 inverted microscope as platform, equipped with an Olympus Plan-Apo 100×, 1.4 NA objective lens. Cells were fixed with 2% paraformaldehyde, washed in PBS, and imaged at room temperature using Picoquant SymPhoTime software. $n = 3$; each replication represents the analysis of 5–8 fields of view. a.u., arbitrary units.

structures, treated monocytes were stained with ER-Tracker Red and observed at various time points over a course of 3 h (Fig. 3). THP-1 cells treated with VLDL lipolysis products (200 mg TG/dl VLDL and 2 U/ml LpL) between 0.5 and 3 h show the gradual accumulation of lipid droplets within the cells, with the greatest number of lipid droplets observed by 3 h clearly seen by DIC (Fig. 3*A*, *first column*). ER-Tracker Red dye (Fig. 3*A*, *middle column*) displays a punctate cytoplasmic localization early in the time course (0.5–1 h), consistent with ER localization. As lipid droplets form, most noticeably at 2 and 3 h, they appear to associate with ER membranes (white arrows). Specifically, at 2 h, you can see that the ER-Tracker Red dye is largely localized to one area where a lipid droplet is located within the cell. By 3 h, the ER-Tracker Red dye appears to surround the periphery of the lipid droplet and is highly concentrated in close proximity to one side of the lipid droplet. This finding is consistent with the idea that neutral lipids coalesce within the ER bilayer into a sphere that eventually buds into the cytosol, a model largely accepted in the lipid droplet field, but is nonetheless unproven (18). A merge of the two images is presented in Fig. 3*A*.

To determine whether other cellular organelles could be involved in lipid droplet biosynthesis, VLDL lipolysis product-treated THP-1 monocytes were stained with Lyso-Tracker Red DND-99 (Supplemental Fig. 2*B*) and Mito-Tracker Green FM (Supplemental Fig. 2*E*) to stain lysozomes and mitochondria, respectively. Neither stain appeared to strongly colocalize with the lipid droplets (Supplemental Fig. 2*C*, 2*F*, black arrows), suggesting that these structures are not involved in lipid droplet formation.

To further investigate the cellular origin of the lipid droplets and confirm their association with the ER, we examined thin sections of VLDL lipolysis product-treated THP-1 monocytes by TEM after 0.5 and 3 h. Fig. 3*B* shows that small lipid droplets (arrows) are visible as early as 30 min after treatment (×8510 total magnification). After 3 h, the droplets appear to be larger in size (Fig. 3*C*, ×8510 total magnification), perhaps because of fusion of multiple smaller droplets within the cell. However, the mechanism that results in this increase in droplet size remains to be elucidated (18). Increased magnification revealed that the lipid droplets are indeed variable in size after 3 h of lipolysis product treatment (Fig. 3*D*, ×15,900 total magnification), and TEM confirms that the lipid droplets are found opposed to the ER, which supports the idea that the lipid droplets likely bud off from the ER during their generation (Fig. 3*E*, ×11,000 total magnification).

Albumin binding to fatty acids released from lipolysis of VLDL attenuates lipid droplet formation and cytokine expression

To determine whether fatty acids released from hydrolysis of VLDL are involved in lipid droplet formation in THP-1 monocytes, we used fatty acid-free BSA to sequester the fatty acids prior to monocyte treatment. After a 2-h treatment, monocytes were stained with Oil Red O and counted as positive or negative for lipid droplets by phase-contrast microscopy. Fig. 4*A* shows that <10% of untreated monocytes contained lipid droplets. Adding BSA to the untreated culture medium had no effect on lipid droplet formation. Treatment with LpL or VLDL, negative controls, did not result in a significant change in lipid droplet formation with or without BSA. However, 80% of monocytes treated with VLDL lipolysis products contained lipid droplets, a significant increase from the controls. Allowing BSA to bind to fatty acids released from the lipolysis of VLDL significantly decreased the number of lipid droplet-laden monocytes (50%, $p < 0.05$), suggesting that free fatty acids, unbound to albumin, play an important role in lipid droplet formation in THP-1 monocytic cells.

Another consequence of monocyte treatment with VLDL lipolysis products was increased cytokine expression. A natural monocytic response to pathogens or toxins is the release of cytokines and chemokines, to ultimately mount an acute inflammatory defense. Such monocyte activation by nonforeign stimuli, such as modified lipids, has been described as an initiating event in atherogenesis (19–21). Fig. 4*B* illustrates that TNF-α, IL-1β, and IL-8 gene expression significantly increased in THP-1 cells after lipolysis product treatment. Furthermore, sequestering lipolytically released fatty acids with BSA, and therefore reducing the number of lipid droplets within the cell, attenuated this cytokine expression. This observation suggests that lipid overload within the cell triggers inflammatory signaling pathways that could result in cellular activation.

In addition, to ensure that our treatment time of 3 h adequately represented the inflammation induced postprandially, TNF-α protein secretion from THP-1 monocytes treated with VLDL lipolysis products for 3, 6, and 24 h was measured by ELISA. The highest secreted TNF-α protein levels were observed after 3 h (86.4 pg/ml versus 65.4 and 62.2 pg/ml after 6 and 24 h, respectively), confirming that our in vitro replication of the peak postprandial period is accurate (data not shown).

Synthetic fatty acids induce lipid droplet formation

Lipolysis of VLDL results in the release of large quantities of nonesterified fatty acids (NEFAs) (22), which have the potential to affect monocytes through a variety of mechanisms. To confirm that fatty acids induce lipid droplet formation, THP-1 monocytes were treated with commercially available unsaturated fatty acids (linoleic acid, 18:2 η-6, and oleic acid, 18:1), and saturated fatty acids (stearic acid, 18:0, and palmitic acid, 16:0). The treatment medium also contained 10% serum albumin. Monocytes were observed under phase-contrast

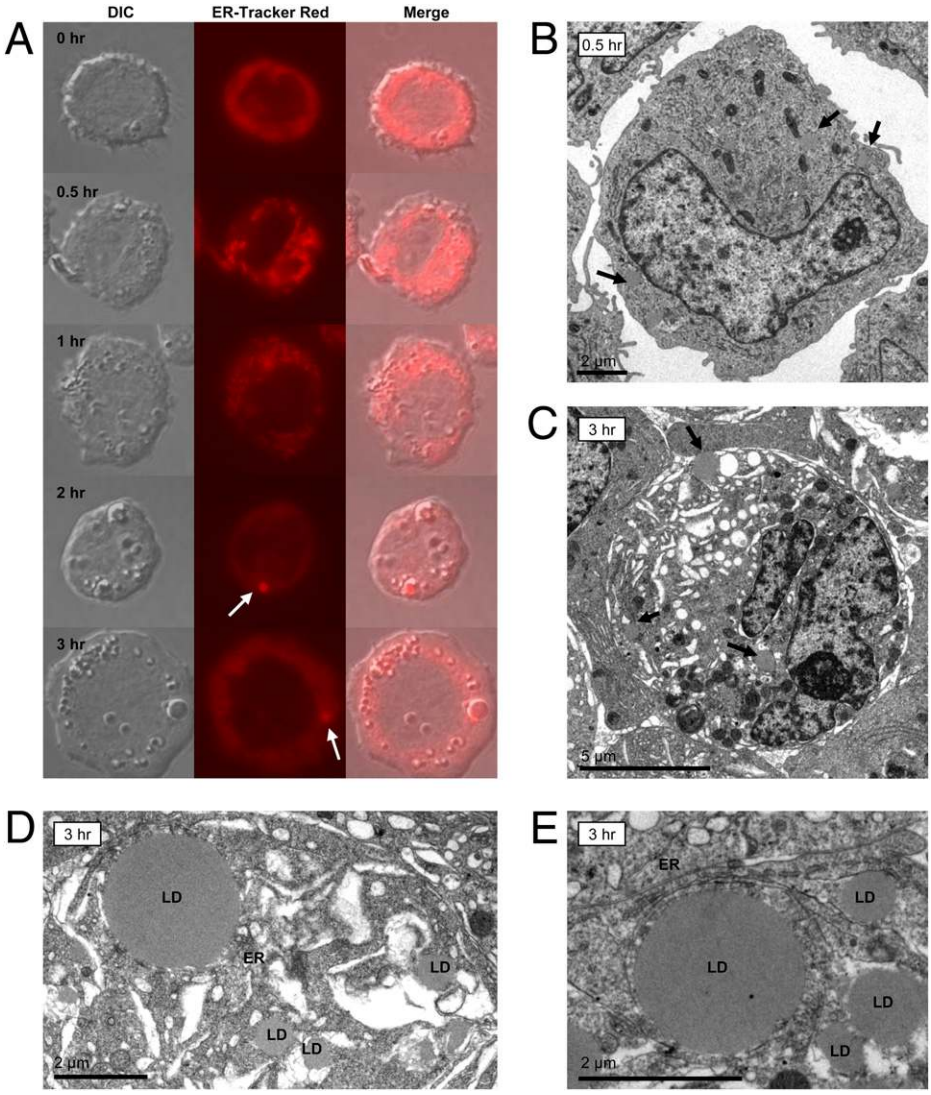

FIGURE 3. VLDL lipolysis product-induced lipid droplets are found in close proximity to the ER. *A*, THP-1 monocytes were treated at a cell density of 1×10^6 cells/ml with VLDL and LpL (200 mg TG/dl, 2 U/ml) over a time course ranging from 0.5 to 3 h. At each time point, cells were collected and stained with ER-Tracker Red to observe any interactions between ER structures and lipid droplet formation. Monocytes were observed using a Zeiss Axioskop2 plus microscope with a *Pan*-Neofluar 40× objective, 1.3 oil. Images were captured using a Zeiss AxioCam MRm camera and processed using AxioVisionLE software. Fluorescence and DIC images of the same cells are shown. At 2 h, ER-associated contents are seen in the same area as some of the lipid droplets within the cell (ER-Tracker Red, arrow). By 3 h, the ER appears to surround the lipid droplet and/or its contents (arrow). Cells from each treatment were analyzed over a minimum of 10 frames per experiment. The experiment was repeated three times, with similar results. *B–E*, TEM of THP-1 monocytes treated with VLDL and LpL (200 mg TG/dl, 2 U/ml) for either 0.5 or 3 h. Monocytes were harvested, prepared for TEM analysis, and embedded in epoxy resin for ultra thin sectioning. The images were collected on a Phillips CM120 microscope at 80 kV using a Gatan MegaScan model 794/20 digital camera. *B*, Monocyte treated with VLDL lipolysis products for 0.5 h contains small, disperse lipid droplets (original magnification ×8510, arrows). *C*, Monocyte treated with VLDL lipolysis products for 3 h contains larger lipid droplets (original magnification ×8510, arrows). *D* and *E*, Higher magnification images of monocytes treated with VLDL lipolysis products for 3 h reveal lipid droplets of multiple sizes (*D*, original magnification ×15,900) and lipid droplets in close proximity to the ER (*E*, original magnification ×11,000). ER, endoplasmic reticulum; LD, lipid droplet.

microscopy after treatment with 150 μM of each fatty acid, which is within the physiological range of NEFAs for humans (23). Lipid droplets were abundant in monocytes treated with each fatty acid as seen in Fig. 5. Linoleic acid (Fig. 5*A*), oleic acid (Fig. 5*B*), and stearic acid (Fig. 5*C*) treatment resulted in the lowest incidence of droplet formation with 53.9%, 50.4%, and 57.8% of total monocytes displaying lipid droplets, respectively, represented quantitatively in Fig. 5*E*. Palmitic acid treatment ultimately generated the highest percentage of lipid droplet-containing cells (Fig. 5*D*, 76.9%), and the droplets that formed within palmitic acid-treated monocytes appeared larger in size than droplets inside cells from any other treatment. This higher incidence of lipid droplet formation from palmitic acid treatment was found to be statistically significant ($p < 0.05$).

Interactions with lipolysis products from FVLDL or PVLDL change the lipid composition of lipid droplets

To determine whether lipolysis products from FVLDL or PVLDL have an influence on the lipid composition of monocyte droplets, we acquired Raman spectra from lipid droplets across the entire Raman-active range from ~400 cm^{-1} to 3100 cm^{-1} using a laser tweezers Raman microscope. This instrument allows us to optically trap monocytes in culture by their cytoplasmic lipid droplets, thereby immobilizing the lipid droplet in the tightly focused laser spot for the duration of the experiment (typically 30–60 s per lipid droplet). In Fig. 6, we show Raman spectra representing the average of several lipid droplets from monocytes that underwent each treatment. All spectra are dominated by the vibrational signature of lipids, indicating

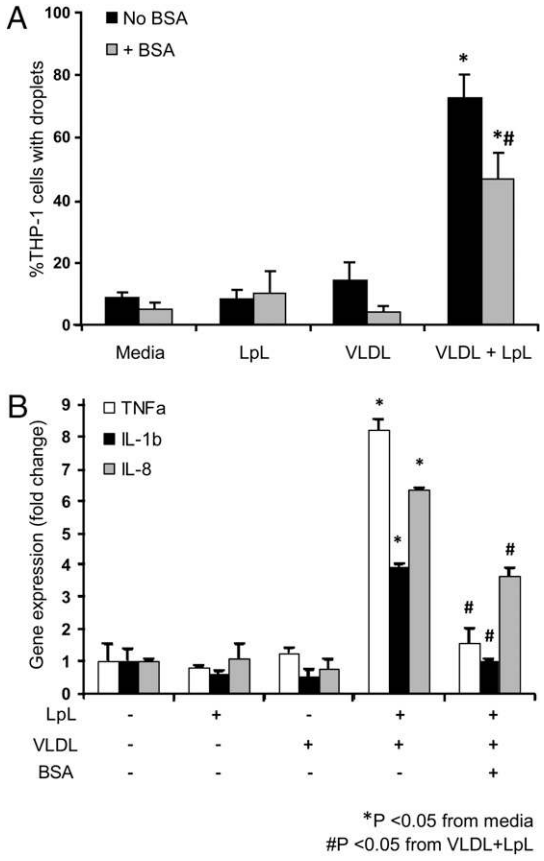

FIGURE 4. Binding fatty acids with BSA partially attenuates lipid droplet formation in THP-1 monocytes. Lipolysis of VLDL was allowed for 30 min at 37˚C, fatty acid-free BSA was added for 5 min, then the combined treatment was applied to THP-1 monocytes for 3 h. *A*, Monocytes were fixed, stained with Oil Red O, and imaged by phase-contrast microscopy using a 60× objective. Monocytes treated with media, LpL (2 U/ml), and VLDL (200 mg TG/dl) with and without BSA (60 mg/ml) were used as negative controls. Cells positive for lipid droplets in each treatment were counted, and expressed as a percentage of cells containing lipid droplets, $n = 5$. A minimum of 300 cells were counted for each treatment. *B*, Gene expression of cytokines TNF-α, IL-1β, and IL-8 measured from THP-1 monocytes treated with the previously described treatments, normalized to media treatment and presented as fold change ± SEM. *Values are significantly different from media control, $p < 0.05$. #Values are significantly different from the VLDL and LpL treatment without BSA, $p < 0.05$.

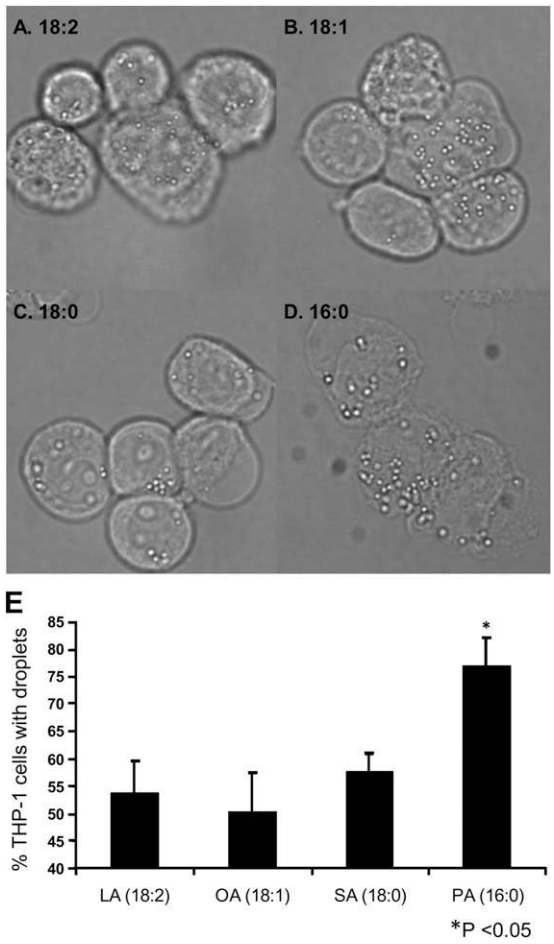

FIGURE 5. Synthetic fatty acids induce formation of lipid droplets in THP-1 monocytes. THP-1 monocytes were treated at a cell density of 1×10^6 cells/ml with linoleic acid (*A*, [18:2], η-6), oleic acid (*B*, [18:1]), stearic acid (*C*, [18:0]), or palmitic acid (*D*, [16:0]) at final concentrations of 150 μM for 3 h. Monocytes were observed by phase-contrast microscopy using an Olympus BX41 microscope with a 60× objective, NA 0.80. Images were captured using an Olympus QColor3 camera and processed using QCapture software. A minimum of 300 cells were counted from each treatment, and the average percentage of cells positive for lipid droplets is represented in *E* ($n = 3$, $*p < 0.05$). Original magnification ×600 for all panels.

that the monocytes were indeed trapped by their lipid droplets. These peaks correspond to the following assignments: Raman peaks of acyl chains in the 1000–1200 cm^{-1} range are typically due to C-C stretching vibration. Specifically, peaks at 1066, 1076, and 1129 cm^{-1} are known to be very sensitive indicators of acyl chain order in lipids. These peaks usually indicate close chain packing typical of the structure of saturated fatty acids at room temperature.

To quantitatively analyze the lipid contents of these droplets, we normalized all the peak vibrations to the 1442 cm^{-1} CH deformation mode, which indicates total lipid content. Specifically, recent articles have established that the ratio of the peak intensity of the 1654 cm^{-1} C-C stretch mode to the 1442 cm^{-1} general lipid vibration provides an excellent quantitative measure of the degree of unsaturation in intracellular lipid droplets (24–26). By carefully comparing these modes between the different samples, it can be seen that monocytes treated with postprandial VLDL have an elevated intensity at the 1129 cm^{-1} mode (I_{1129}/I_{1445}: PVLDL: 0.16 ± 0.01, FVLDL: 0.08 ± 0.01, PVLDL and LpL: 0.11 ± 0.01, FVLDL and LpL: 0.08 ± 0.01). This ratio is similar to that obtained directly from PVLDL lipoproteins and indicates that their saturated fatty acid core is likely being incorporated in its entirety into intracellular lipid droplets (24). Interestingly, the observation is quite different when the total degree of unsaturation is calculated (ratio I_{1654}/I_{1445}: PVLDL: 0.46 ± 0.04, FVLDL: 0.50 ± 0.04, PVLDL and LpL: 0.57 ± 0.05, FVLDL and LpL: 0.65 ± 0.05). In this study, treatment with lipolysis products leads to significantly higher degrees of unsaturation, suggesting that monocytes are trying to compensate the lipotoxic effects of exposure to saturated fatty acids. Interestingly, the TG content in all cells is relatively unchanged and rather similar (ratio I_{1740}/I_{1445}: PVLDL: 0.08 ± 0.01, FVLDL: 0.07 ± 0.01, PVLDL and LpL: 0.11 ± 0.01, FVLDL and LpL: 0.12 ± 0.01). Based on these observations, it is quite apparent that lipid droplets in monocytes treated with PVLDL lipolysis products contain on average ~15% more saturated lipids than those from FVLDL lipolysis product-treated monocytes.

Lipid droplets are present in primary human monocytes after consumption of a high-fat meal

To eliminate the possibility that the cytotoxic response of THP-1 monocytes to VLDL lipolysis products is an in vitro effect, we examined freshly isolated human monocytes before and after the

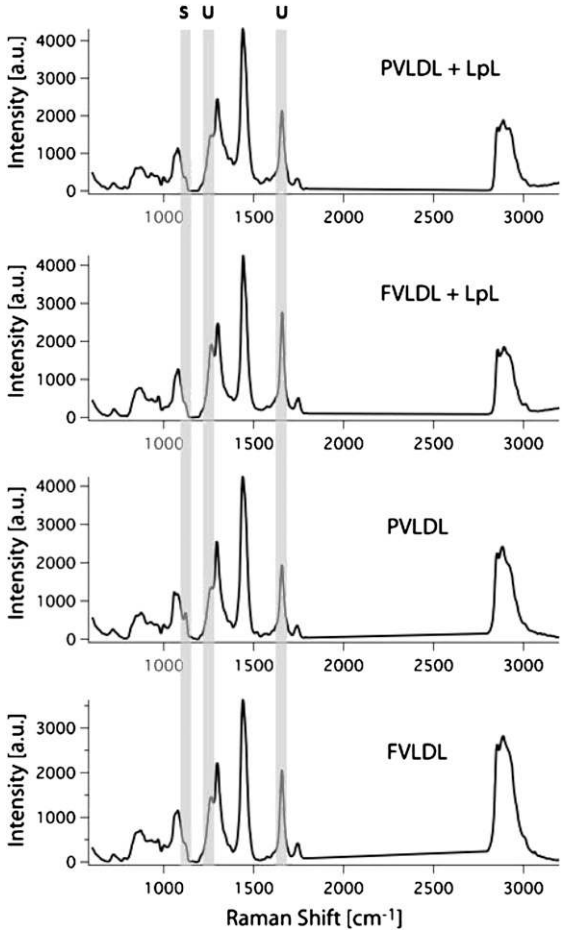

FIGURE 6. Lipid droplets in THP-1 monocytes exposed to fasting or PVLDL lipolysis products exhibit distinct differences in their lipid composition. THP-1 monocytes were treated at a cell density of 1×10^6 cells/ml with either VLDL or VLDL and LpL (200 mg TG/dl, 2 U/ml) for 3 h with VLDL obtained in the fasting and the postprandial states. THP-1 monocytes were also treated with FVLDL and PVLDL alone (in the absence of LpL). On average, 10 Raman spectra from cells treated with the different products were obtained and their signal intensities were averaged ($n = 3$). Raman markers for saturation (1129 cm^{-1}) and unsaturation (1266 cm^{-1} and 1654 cm^{-1}) are highlighted by gray bars. a.u., arbitrary units.

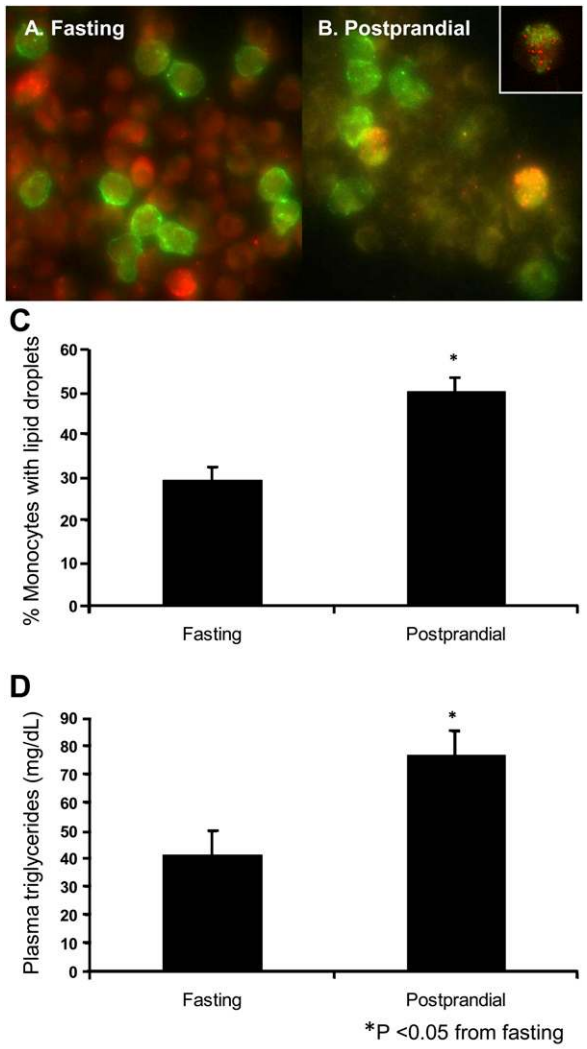

FIGURE 7. The postprandial state induces lipid droplet formation in freshly isolated human monocytes. *A* and *B*, Peripheral blood was drawn before and after consumption of a moderately high-fat meal from 10 healthy human volunteers. Monocytes were labeled with CD14-FITC, fixed, and stained with Oil Red O. Fasting (*A*) and postprandial monocytes (*B*) were imaged using a Δ Vision Deconvolution microscope with a 60× objective. CD14-positive monocytes are shown in green, whereas Oil Red O-stained lipid droplets appear red. Inset of *B*, A CD14-positive monocyte that contains lipid droplets is shown at 2× digital magnification. *C*, Percent cells containing lipid droplets was calculated by analyzing 40 frames from each sample, with a minimum of 150 cells counted from each fasting and postprandial time point for each subject. 50.3 ± 3.1% of postprandial monocytes contained lipid droplets, compared with 29.4 ± 3.0% of monocytes during the fasting state. *D*, Postprandial blood plasma TG levels (77.0 ± 8.3 mg TG/dl) were also higher compared with fasting blood samples (41.5 ± 8.3 mg TG/dl), averaged from 10 subject samples. $*p < 0.05$. Original magnification ×600 for *A* and *B*.

consumption of a moderately high-fat meal. Monocytes were labeled with a CD14 Ab, a cell surface marker found exclusively on monocytes, conjugated to the fluorescent dye Alexa488 that renders all monocytes fluorescent green. Monocytes were fixed and subsequently stained with Oil Red O for lipid droplet visualization at red wavelengths. Monocytes isolated from fasting blood contained few red-stained lipid droplets (Fig. 7*A*), whereas cells isolated from postprandial blood contained more lipid droplet-positive monocytes (Fig. 7*B*). Monocytes positive for lipid droplets, that is, cells that stained green and contained punctate red droplets, were counted and expressed as a percentage of total monocytes. In this study, comparing the responses of 10 randomly selected healthy volunteers, 29.4% of fasting monocytes contained lipid droplets, compared with 50.3% of postprandial monocytes (Fig. 7*C*). Similarly, when THP-1 monocytes were treated with fasting or postprandial plasma at the same average TG concentrations expressed by our donors (42 and 79 mg TG/dl, respectively), the percentage of cells positive for lipid droplets (33.5% fasting and 70.0% postprandial, data not shown) closely mimicked the trend observed using fresh monocytes. The red cells in Fig. 7*A* are nonmonocytic leukocytes that have picked up the Oil Red O stain. Note that most of these cells are uniformly stained red, with few punctate red spots, suggesting that Oil Red O stains plasma membrane lipids of all cells. However, in Fig.7*A* there are a few nonmonocytic leukocytes that stain brightly red in a speckled pattern, which suggests that some unidentified nonmonocytic leukocytes also develop lipid droplets. In Fig. 7*B*, we believe that the absence of red nonmonocytic leukocytes is due to the chosen focal plane in this particular frame, in which the monocytes are in focus and the underlying nonmonocytic leukocytes are below the plane of focus. This, and the brightness of the red droplets within the monocytes,

renders the Oil Red O signal from the nonmonocytic leukocytes slightly dampened.

Because the postprandial period chosen coincides with the average spike in TGs seen after ingestion of a high-fat meal, as shown in Fig. 7*D*, it appears that circulating TGs or their lipolysis products induce lipid droplet formation within monocytes in vivo. The average NEFA levels of the fasting and postprandial plasma were 0.242 mmol/l and 0.301 mmol/l, respectively. In addition, the 10 blood donors had an average postprandial TG level of 79 mg/dl. Because this value is lower than the TG levels used in our previous treatments, we repeated the initial THP-1 monocyte treatment with VLDL lipolysis products at this TG concentration (data not shown). The loading capacity at 79 mg TG/dl was quantified as 69% of total THP-1 monocytes containing lipid droplets, slightly lower than the 200 mg/dl dose depicted in Fig. 4 (80% positive for droplets).

As an additional link to monocyte inflammation, a previous study from our laboratory showed that the peak postprandial period also coincided with increased levels of TNF-α and IL-1β secretion from circulating monocytes (3). To confirm that lipid droplet formation in fresh monocytes also correlates with an inflammatory response, we isolated PBMCs from fasting and 3.5-h postprandial blood and measured cytokine gene expression. As shown in Supplemental Fig. 3, PBMC expression levels of TNF-α, IL-1β, and IL-8 significantly increased during the peak postprandial period, confirming our previous observation.

Discussion

The aims of this study were to identify and characterize the cytosolic lipid droplets that form in monocytes in response to incubation with lipolysis products from VLDL and to determine how this effect relates to postprandial hypertriglyceridemia. Controlled lipid storage is a known function of monocyte-derived macrophages, but to our knowledge has not been investigated in undifferentiated monocytes. We found that monocytes in culture and freshly isolated primary monocytes display similar lipid droplet formation when exposed to PVLDL lipolysis products, suggesting that this is not an artifact of cell culture or unique to a particular cell line. Fatty acids released on lipolysis appear to be causative, and the level of unsaturation of these fatty acids is critical for their rate of formation and the size to which the droplets can grow. Furthermore, these lipid droplets appear to originate from the ER as previously suggested, in agreement with the current lipid droplet model.

Lipid droplet physiology has been the subject of intense research for many years, but gaps in the knowledge base remain. Specifically, although polyunsaturated fatty acids have been established as major stimuli for lipid droplet formation (27), it remains unknown what function these droplets have in cells that do not normally store large amounts of lipid, such as monocytes. In addition, a concise mechanism describing fatty acid uptake and repackaging into TG-filled droplets by immune cells is unknown.

Previous research has shown that neutral lipid storage is important for cellular defense. Excess fatty acids are toxic to cells, but unsaturated fatty acids have been shown to protect normal cells against the damage induced by saturated fatty acids (28). One possible reason that lipid droplets form in response to VLDL lipolysis products is to prevent lipotoxicity, which has clinical relevance in human disease. The cellular mechanisms by which lipid-laden cells tolerate lipid overload or undergo lipotoxicity are not well known. Recently, Cnop et al. showed that pancreatic islet cells treated with oleate were able to survive lipotoxicity by forming lipid droplets, whereas cells that did not survive the treatment did not contain droplets (29). In our study, THP-1 monocytes formed lipid droplets in response to polyunsaturated, monounsaturated, and saturated fatty acids, while maintaining cell viability. In a previous study, we determined that lipolysis of VLDL from healthy individuals releases a combination of fatty acids of which palmitic acid (120 ± 19 nmol/mg TG), stearic acid (23.8 ± 6.3 nmol/mg TG), oleic acid (67.8 ± 10 nmol/mg TG), and linoleic acid (48.2 ± 11 nmol/mg TG) were the most abundant (22). Exposure of monocytes to this combination of saturated and unsaturated NEFAs results in the formation of lipid droplets. We can speculate that the sequestration of long-chain fatty acids into droplets prevents them from initiating proapoptotic signaling cascades and/or generating reactive oxygen species, two endpoints of lipotoxicity.

We have shown that the saturated fatty acid palmitic acid leads to the highest level of lipid droplet formation, but likely at the expense of long-term cell viability. Higa et al. showed that palmitate increased TG accumulation in pancreatic β cells, presumably by forming lipid droplets, but this lipid accumulation was not linked to subsequent apoptosis at high-palmitate concentrations (30). A continuous dose-dependent Akt phosphorylation in those cells suggests that the accumulated lipid droplets triggered cell survival pathways through Akt. However, at higher doses of palmitate the cells became apoptotic, suggesting that either lipid droplet-induced survival signaling can reach a threshold, or that the cells switched over to a proapoptotic pathway. Similarly, Listenberger et al. showed that Chinese hamster ovary cells treated with palmitate did not accumulate TG and became apoptotic, whereas cells treated with oleate did accumulate lipids and survived lipotoxicity (28). They reasoned that the accumulation of TG protected the cells from apoptosis, implying that unsaturated fatty acids protect against lipotoxicity, whereas saturated fatty acids promote it. In contrast, our study shows that lipid droplets form after monocyte treatment of both saturated and unsaturated fatty acids. It is possible that our treatment dose of 150 μM, palmitic acid was able to accumulate in lipid droplets, whereas the higher treatment concentrations reported by Listenberger et al. yielded different results. In addition, the treatment times varied, which could also explain the discrepancies between studies.

It has previously been reported that sites of inflammation inside the human body, such as arthritic joints or asthmatic bronchi, contain cells with lipid droplets (31, 32). This suggests that lipid droplets may play a role in regulating or responding to inflammation. Previous results reported by Bozza et al. showed that lipid body formation could be inhibited by aspirin and nonsteroidal anti-inflammatory drugs, indicating that cyclooxygenase-2 and its downstream eicosanoid and PG targets are involved (33). Cyclooxygenase-2 and PGs also have been found inside lipid bodies from neutrophils, eosinophils, mast cells, and adenocarcinoma cell lines (34–36). Haversen et al. showed that long-chain fatty acids, such as palmitate and stearate, induced the mRNA expression and secretion of inflammatory mediators TNF-α, IL-1β, and IL-8 from monocyte-derived macrophages, but linoleate did not induce cytokine secretion (37). The fact that these two saturated fatty acids are abundantly released from hydrolysis of our VLDL, they both initiate lipid droplet formation, and have been shown to elicit an inflammatory response from monocyte-derived macrophages suggests that they are primary activating agents in our system. We have demonstrated herein that VLDL lipolysis products initiate a proinflammatory response from monocytes, which becomes attenuated when the stimulus to lipid droplet formation is blocked. An important question that remains is whether there is a cause-and-effect relationship between the monocyte proinflammatory state and droplet formation.

In an effort to determine the origin of lipid droplets in monocytes, we stained specific organelles to determine whether they colocalize with lipid droplets present. Based on the comparison between fluorescence from these organelle-specific stains and DIC images, it appears that there is a time-dependent association with ER. Lipid

droplets that originate from the ER may be too small to be captured by current microscopic techniques, and remain unassociated from the ER, while they become large enough to detect (38). TEM images of VLDL lipolysis product-treated monocytes show lipid droplets in close proximity to the ER membrane. The notion that lipid droplets arise as specialized regions of the ER is attractive, given that in times of metabolic stress this would facilitate the rapid exchange of lipids and proteins. However, the possibility of an endosomal trafficking mechanism also exists regarding the formation of lipid droplets. Fatty acids have been shown to induce the internalization and endosomal association of caveolin-1 and fatty acid-binding proteins, which normally reside in membrane regions termed caveolae (39, 40). In addition, it has been shown that caveolin-1 associates with lipid droplets and can directly bind fatty acids (41), suggesting that the lipid droplet contents originate from outside of the cell, which could be the case in our study.

We observed profound effects on the overall lipid composition of lipid droplets after treatment with lipolysis products from FVLDL versus PVLDL. The postprandial period, as experienced multiple times per day, is often characterized by increased levels of circulating TGs and fatty acids (42, 43), and also by activated monocytes (3). As evidenced by Raman spectroscopic analyses of individual intracellular lipid droplets, exposure to lipolysis products from PVLDL resulted in a higher level of saturation (15%) inside the lipid droplets, which is likely to invoke a stronger lipotoxic response. In support of this result, Chan et al. have shown that VLDL isolated from the same population of fasting subjects has a lower saturated fatty acid content than PVLDL (24). Overall, our results suggest that a higher saturated-to-unsaturated fat ratio in PVLDL contributes to increased monocyte lipid droplet formation during the peak postprandial period, potentially representing an activating event leading to monocyte recruitment to the vascular wall.

Although the formation of lipid droplets in a monocyte cell line in response to VLDL lipolysis product exposure is an interesting observation, it was important to establish physiological relevance. By conducting a study with randomly selected healthy volunteers, we confirmed the presence of lipid droplets in their monocytes before and 3.5 h after the consumption of a moderately high-fat meal. We found that these subjects exhibited an increase in plasma TGs 3–4 h after meal consumption, as has been previously reported (43, 44), and which coincides with the peak monocyte inflammatory response (3). We speculated that, as seen in vitro, elevated VLDL lipolysis products could induce lipid droplet formation within circulating monocytes in vivo. In this study, we report for the first time that monocytes isolated from human subjects during the peak postprandial period contain lipid droplets. A similar finding has recently been reported in hypercholesterolemic apoE knockout mice (45), from which $CD11c^+$ monocytes contained lipid droplets, whereas the same monocytic population from wild-type mice did not. This monocytic response to a high-fat meal could be even more pronounced in humans with dyslipidemias, such as combined dyslipidemia.

In this study, we have conclusively determined that monocytes treated with PVLDL lipolysis products generate droplets that are in fact lipid-filled, form due to interactions with free fatty acids, are likely to originate from the ER, and are found both in vitro and more importantly in vivo. Furthermore, we speculate that these lipid droplets form to prevent lipotoxicity. We have also established that both unsaturated and saturated fatty acids induce lipid droplet formation, but that the increased number of cells containing lipid droplets seen postprandially could be linked to a higher saturated-to-unsaturated fatty acid ratio in PVLDL. The identification of lipid droplets inside human monocytes could provide a novel biomarker for stratification of risk for ASCVD in the future.

Acknowledgments

We thank J. Engebrecht (University of California, Davis) and S. Dandekar (University of California, Davis) for use of their microscopes to complete this work, as well as G. Adamson and P. Kysar for technical assistance in the Electron Microscopy Laboratory, Department of Pathology and Laboratory Medicine, University of California, Davis. We also thank G. McNerny for technical assistance with the Δ Vision deconvolution microscope, and T. Weeks and I. Schie for help in acquiring monocyte CARS images.

Disclosures

The authors have no financial conflicts of interest.

References

1. Kelley, J. L., M. M. Rozek, C. A. Suenram, and C. J. Schwartz. 1988. Activation of human peripheral blood monocytes by lipoproteins. *Am. J. Pathol.* 130: 223–231.
2. Alipour, A., A. J. van Oostrom, A. Izraeljan, C. Verseyden, J. M. Collins, K. N. Frayn, T. W. Plokker, J. W. Elte, and M. Castro Cabezas. 2008. Leukocyte activation by triglyceride-rich lipoproteins. *Arterioscler. Thromb. Vasc. Biol.* 28: 792–797.
3. Hyson, D. A., T. G. Paglieroni, T. Wun, and J. C. Rutledge. 2002. Postprandial lipemia is associated with platelet and monocyte activation and increased monocyte cytokine expression in normolipemic men. *Clin. Appl. Thromb. Hemost.* 8: 147–155.
4. Eiselein, L., D. W. Wilson, M. W. Lamé, and J. C. Rutledge. 2007. Lipolysis products from triglyceride-rich lipoproteins increase endothelial permeability, perturb zonula occludens-1 and F-actin, and induce apoptosis. *Am. J. Physiol. Heart Circ. Physiol.* 292: H2745–H2753.
5. Fujimoto, T., Y. Ohsaki, J. Cheng, M. Suzuki, and Y. Shinohara. 2008. Lipid droplets: a classic organelle with new outfits. *Histochem. Cell Biol.* 130: 263–279.
6. Murphy, D. J. 2001. The biogenesis and functions of lipid bodies in animals, plants and microorganisms. *Prog. Lipid Res.* 40: 325–438.
7. Fujimoto, T., and Y. Ohsaki. 2006. Cytoplasmic lipid droplets: rediscovery of an old structure as a unique platform. *Ann. N. Y. Acad. Sci.* 1086: 104–115.
8. Martin, S., and R. G. Parton. 2006. Lipid droplets: a unified view of a dynamic organelle. *Nat. Rev. Mol. Cell Biol.* 7: 373–378.
9. Welte, M. A. 2007. Proteins under new management: lipid droplets deliver. *Trends Cell Biol.* 17: 363–369.
10. Murphy, D. J., and J. Vance. 1999. Mechanisms of lipid-body formation. *Trends Biochem. Sci.* 24: 109–115.
11. Brown, D. A. 2001. Lipid droplets: proteins floating on a pool of fat. *Curr. Biol.* 11: R446–R449.
12. Novikoff, A. B., P. M. Novikoff, O. M. Rosen, and C. S. Rubin. 1980. Organelle relationships in cultured 3T3-L1 preadipocytes. *J. Cell Biol.* 87: 180–196.
13. Tauchi-Sato, K., S. Ozeki, T. Houjou, R. Taguchi, and T. Fujimoto. 2002. The surface of lipid droplets is a phospholipid monolayer with a unique Fatty Acid composition. *J. Biol. Chem.* 277: 44507–44512.
14. Le Lay, S., and I. Dugail. 2009. Connecting lipid droplet biology and the metabolic syndrome. *Prog. Lipid Res.* 48: 191–195.
15. Cohn, J. S., D. A. Wagner, S. D. Cohn, J. S. Millar, and E. J. Schaefer. 1990. Measurement of very low density and low density lipoprotein apolipoprotein (Apo) B-100 and high density lipoprotein Apo A-I production in human subjects using deuterated leucine. Effect of fasting and feeding. *J. Clin. Invest.* 85: 804–811.
16. Kota, R. S., C. V. Ramana, F. A. Tenorio, R. I. Enelow, and J. C. Rutledge. 2005. Differential effects of lipoprotein lipase on tumor necrosis factor-alpha and interferon-gamma-mediated gene expression in human endothelial cells. *J. Biol. Chem.* 280: 31076–31084.
17. Kota, R. S., J. C. Rutledge, K. Gohil, A. Kumar, R. I. Enelow, and C. V. Ramana. 2006. Regulation of gene expression in RAW 264.7 macrophage cell line by interferon-gamma. *Biochem. Biophys. Res. Commun.* 342: 1137–1146.
18. Listenberger, L. L., and D. A. Brown. 2008. Lipid droplets. *Curr. Biol.* 18: R237–R238.
19. Ross, R. 1999. Atherosclerosis—an inflammatory disease. *N. Engl. J. Med.* 340: 115–126.
20. Osterud, B., and E. Bjorklid. 2003. Role of monocytes in atherogenesis. *Physiol. Rev.* 83: 1069–1112.
21. Greaves, D. R., and K. M. Channon. 2002. Inflammation and immune responses in atherosclerosis. *Trends Immunol.* 23: 535–541.
22. Wang, L., R. Gill, T. L. Pedersen, L. J. Higgins, J. W. Newman, and J. C. Rutledge. 2009. Triglyceride-rich lipoprotein lipolysis releases neutral and oxidized FFAs that induce endothelial cell inflammation. *J. Lipid Res.* 50: 204–213.
23. Plaisance, E. P., P. W. Grandjean, R. L. Judd, K. W. Jones, and J. K. Taylor. 2009. The influence of sex, body composition, and nonesterified fatty acids on serum adipokine concentrations. *Metabolism* 58: 1557–1563.
24. Chan, J. W., D. Motton, J. C. Rutledge, N. L. Keim, and T. Huser. 2005. Raman spectroscopic analysis of biochemical changes in individual triglyceride-rich lipoproteins in the pre- and postprandial state. *Anal. Chem.* 77: 5870–5876.
25. Rinia, H. A., K. N. Burger, M. Bonn, and M. Müller. 2008. Quantitative label-free imaging of lipid composition and packing of individual cellular lipid droplets using multiplex CARS microscopy. *Biophys. J.* 95: 4908–4914.

26. Le, T. T., H. M. Duren, M. N. Slipchenko, C. D. Hu, and J. X. Cheng. 2009. Label-free quantitative analysis of lipid metabolism in living Caenorhabditis elegans. *J. Lipid Res.* doi:10.1194/jlr.D000638.
27. Fujimoto, Y., J. Onoduka, K. J. Homma, S. Yamaguchi, M. Mori, Y. Higashi, M. Makita, T. Kinoshita, J. Noda, H. Itabe, and T. Takanoa. 2006. Long-chain fatty acids induce lipid droplet formation in a cultured human hepatocyte in a manner dependent of Acyl-CoA synthetase. *Biol. Pharm. Bull.* 29: 2174–2180.
28. Listenberger, L. L., X. Han, S. E. Lewis, S. Cases, R. V. Farese, Jr., D. S. Ory, and J. E. Schaffer. 2003. Triglyceride accumulation protects against fatty acid-induced lipotoxicity. *Proc. Natl. Acad. Sci. USA* 100: 3077–3082.
29. Cnop, M., J. C. Hannaert, A. Hoorens, D. L. Eizirik, and D. G. Pipeleers. 2001. Inverse relationship between cytotoxicity of free fatty acids in pancreatic islet cells and cellular triglyceride accumulation. *Diabetes* 50: 1771–1777.
30. Higa, M., M. Shimabukuro, Y. Shimajiri, N. Takasu, T. Shinjyo, and T. Inaba. 2006. Protein kinase B/Akt signalling is required for palmitate-induced beta-cell lipotoxicity. *Diabetes Obes. Metab.* 8: 228–233.
31. Weinstein, J. 1980. Synovial fluid leukocytosis associated with intracellular lipid inclusions. *Arch. Intern. Med.* 140: 560–561.
32. Triggiani, M., A. Oriente, M. C. Seeds, D. A. Bass, G. Marone, and F. H. Chilton. 1995. Migration of human inflammatory cells into the lung results in the remodeling of arachidonic acid into a triglyceride pool. *J. Exp. Med.* 182: 1181–1190.
33. Bozza, P. T., J. L. Payne, S. G. Morham, R. Langenbach, O. Smithies, and P. F. Weller. 1996. Leukocyte lipid body formation and eicosanoid generation: cyclooxygenase-independent inhibition by aspirin. *Proc. Natl. Acad. Sci. USA* 93: 11091–11096.
34. Dvorak, A. M., E. Morgan, R. P. Schleimer, S. W. Ryeom, L. M. Lichtenstein, and P. F. Weller. 1992. Ultrastructural immunogold localization of prostaglandin endoperoxide synthase (cyclooxygenase) to non-membrane-bound cytoplasmic lipid bodies in human lung mast cells, alveolar macrophages, type II pneumocytes, and neutrophils. *J. Histochem. Cytochem.* 40: 759–769.
35. Dvoràk, A. M., E. S. Morgan, D. M. Tzizik, and P. F. Weller. 1994. Prostaglandin endoperoxide synthase (cyclooxygenase): ultrastructural localization to nonmembrane-bound cytoplasmic lipid bodies in human eosinophils and 3T3 fibroblasts. *Int. Arch. Allergy Immunol.* 105: 245–250.
36. Accioly, M. T., P. Pacheco, C. M. Maya-Monteiro, N. Carrossini, B. K. Robbs, S. S. Oliveira, C. Kaufmann, J. A. Morgado-Diaz, P. T. Bozza, and J. P. Viola. 2008. Lipid bodies are reservoirs of cyclooxygenase-2 and sites of prostaglandin-E2 synthesis in colon cancer cells. *Cancer Res.* 68: 1732–1740.
37. Håversen, L., K. N. Danielsson, L. Fogelstrand, and O. Wiklund. 2009. Induction of proinflammatory cytokines by long-chain saturated fatty acids in human macrophages. *Atherosclerosis* 202: 382–393.
38. Hakumäki, J. M., and R. A. Kauppinen. 2000. 1H NMR visible lipids in the life and death of cells. *Trends Biochem. Sci.* 25: 357–362.
39. Trigatti, B. L., R. G. Anderson, and G. E. Gerber. 1999. Identification of caveolin-1 as a fatty acid binding protein. *Biochem. Biophys. Res. Commun.* 255: 34–39.
40. Pol, A., S. Martin, M. A. Fernández, M. Ingelmo-Torres, C. Ferguson, C. Enrich, and R. G. Parton. 2005. Cholesterol and fatty acids regulate dynamic caveolin trafficking through the Golgi complex and between the cell surface and lipid bodies. *Mol. Biol. Cell* 16: 2091–2105.
41. Pol, A., S. Martin, M. A. Fernandez, C. Ferguson, A. Carozzi, R. Luetterforst, C. Enrich, and R. G. Parton. 2004. Dynamic and regulated association of caveolin with lipid bodies: modulation of lipid body motility and function by a dominant negative mutant. *Mol. Biol. Cell* 15: 99–110.
42. Karpe, F. 1999. Postprandial lipoprotein metabolism and atherosclerosis. *J. Intern. Med.* 246: 341–355.
43. Chung, B. H., B. Hennig, B. H. Cho, and B. E. Darnell. 1998. Effect of the fat composition of a single meal on the composition and cytotoxic potencies of lipolytically-releasable free fatty acids in postprandial plasma. *Atherosclerosis* 141: 321–332.
44. Karpe, F., G. Steiner, T. Olivecrona, L. A. Carlson, and A. Hamsten. 1993. Metabolism of triglyceride-rich lipoproteins during alimentary lipemia. *J. Clin. Invest.* 91: 748–758.
45. Wu, H., R. M. Gower, H. Wang, X. Y. Perrard, R. Ma, D. C. Bullard, A. R. Burns, A. Paul, C. W. Smith, S. I. Simon, and C. M. Ballantyne. 2009. Functional role of CD11c+ monocytes in atherogenesis associated with hypercholesterolemia. *Circulation* 119: 2708–2717.